JOURNAL OF BACTERIOLOGY, July 2006, p. 4777–4786 Vol. 188, No. 13
0021-9193/06/$08.00+0 doi:10.1128/JB.00195-06


# Uracil Salvage Pathway in *Lactobacillus plantarum*: Transcription and Genetic Studies

Florence Arsène-Ploetze,[1] Hervé Nicoloff,[1]† Benoît Kammerer,[1] Jan Martinussen,[2] and Françoise Bringel[1]*

*UMR7156 Université Louis Pasteur/CNRS, Génétique Moléculaire, Génomique, Microbiologie, 28 rue Goethe, F-67083 Strasbourg, France,[1] and Biocentrum-DTU, Technical University of Denmark, DK-2800 Kgs. Lyngby, Denmark[2]*

Received 6 February 2006/Accepted 16 April 2006

**The uracil salvage pathway in *Lactobacillus plantarum* was demonstrated to be dependent on the *upp-pyrP* gene cluster. PyrP was the only high-affinity uracil transporter since a *pyrP* mutant no longer incorporated low concentrations of radioactively labeled uracil and had increased resistance to the toxic uracil analogue 5-fluorouracil. The *upp* gene encoded a uracil phosphoribosyltransferase (UPRT) enzyme catalyzing the conversion of uracil and 5-phosphoribosyl-α-1-pyrophosphate to UMP and pyrophosphate. Analysis of mutants revealed that UPRT is a major cell supplier of UMP synthesized from uracil provided by preformed nucleic acid degradation. In a mutant selection study, seven independent *upp* mutants were isolated and all were found to excrete low amounts of pyrimidines to the growth medium. Pyrimidine-dependent transcription regulation of the biosynthetic pyrimidine *pyrR1-B-C-Aa1-Ab1-D-F-E* operon was impaired in the *upp* mutants. Despite the fact that *upp* and *pyrP* are positioned next to each other on the chromosome, they are not cotranscribed. Whereas *pyrP* is expressed as a monocistronic message, the *upp* gene is part of the *lp_2376-glyA-upp* operon. The *lp_2376* gene encodes a putative protein that belongs to the conserved protein family of translation modulators such as Sua5, YciO, and YrdC. The *glyA* gene encodes a putative hydroxymethyltransferase involved in $C_1$ unit charging of tetrahydrofolate, which is required in the biosynthesis of thymidylate, pantothenate, and purines. Unlike *upp* transcription, *pyrP* transcription is regulated by exogenous pyrimidine availability, most likely by the same mechanism of transcription attenuation as that of the *pyr* operon.**

Growing organisms need pyrimidine molecules to synthesize their nucleic acids (DNA and RNA). The pyrimidine needs of living cells are fulfilled either via de novo synthesis or via salvage of preformed pyrimidine bases and nucleosides provided by the surrounding medium (Fig. 1) (23). In the biosynthetic pathway, UMP is formed in six enzymatic steps. In *Lactobacillus plantarum*, the enzymes are encoded by the *pyr* operon with the gene order *pyrR1-B-C-Aa1-Ab1-D-F-E* (9). Uracil salvage is found in *L. plantarum* since a *pyrD* mutant impaired in de novo pyrimidine synthesis was able to use uracil as the sole pyrimidine source (26). The key enzyme in microbial pyrimidine salvage is uracil phosphoribosyltransferase (UPRT) (EC 2.4.2.9), which catalyzes the conversion of uracil and 5-phosphoribosyl-α-1-pyrophosphate (PRPP) to UMP and pyrophosphate. On the *L. plantarum* genome, a putative *upp* gene codes for a protein of 209 residues with significant sequence identity with characterized UPRT: 75% identity with *Lactococcus lactis* UPRT (17) and 68% identity with *Bacillus subtilis* UPRT (16). The *upp* gene was found immediately upstream of the *pyrP* gene (EMBL sequence accession no. AL935263). The *pyrP* gene encodes a putative 426-residue transmembrane protein of the conserved UraA xanthine/uracil permease family (COG2333). In *L. plantarum*, the *upp* and *pyrP* genes are contiguous, oriented in the same direction but separated by a 1.1-kb intergenic region with no detected open reading frames, suggesting the absence of cotranscription of the two genes. This genetic organization is different from previously studied organisms: the *upp* and *uraA* genes are unlinked in *Streptomyces* (GenBank accession no. NC_003888) (13) and form a bicistronic operon in *Escherichia coli* (1), while the *pyrP* gene is cotranscribed with the adjacent *pyrR*/*pyrB* genes in *B. subtilis* (32) and *L. lactis* (18). In these organisms, *pyrP* transcription is regulated in response to pyrimidine availability.

Pyrimidine-dependent repression occurs by a mechanism of transcription attenuation that has been most studied for *B. subtilis* (32) but that also occurs in many other gram-positive bacteria, including *L. plantarum* (26) and *L. lactis* (18). When uracil is present in the culture medium, de novo pyrimidine synthesis is inhibited due to repression of the expression of the pyrimidine biosynthetic genes encoded by the *pyr* operon. The first gene of the *B. subtilis* and *L. plantarum pyr* operon encodes an RNA binding regulator PyrR (called PyrR1 in *L. plantarum*) that represses expression of the downstream *pyr* genes (26). When intracellular UMP concentration is high, the repressor-UMP complex binds the target RNA hexaloop formed at the tip of the anti-antiterminator mRNA hairpin structure in the 5′ leader sequence of regulated genes. Binding of the repressor prevents formation of the antiterminator structure, allowing the terminator RNA loop to be formed and the transcription to be terminated. When the intracellular UMP is low, the repressor remains unbound, favoring formation of the antiterminator RNA loop, preventing terminator loop formation.

* Corresponding author. Mailing address: UMR7156, Université Louis Pasteur/CNRS, Génétique Moléculaire, Génomique, Microbiologie, 28 rue Goethe, F-67083 Strasbourg, France. Phone: 33 3 90 24 18 15. Fax: 33 3 90 24 20 28. E-mail: bringel@gem.u-strasbg.fr.

† Present address: Center for Adaptation Genetics and Drug Resistance, Departments of Molecular Biology and Microbiology, Tufts University School of Medicine, 136 Harrison Ave., Boston, MA 02111.

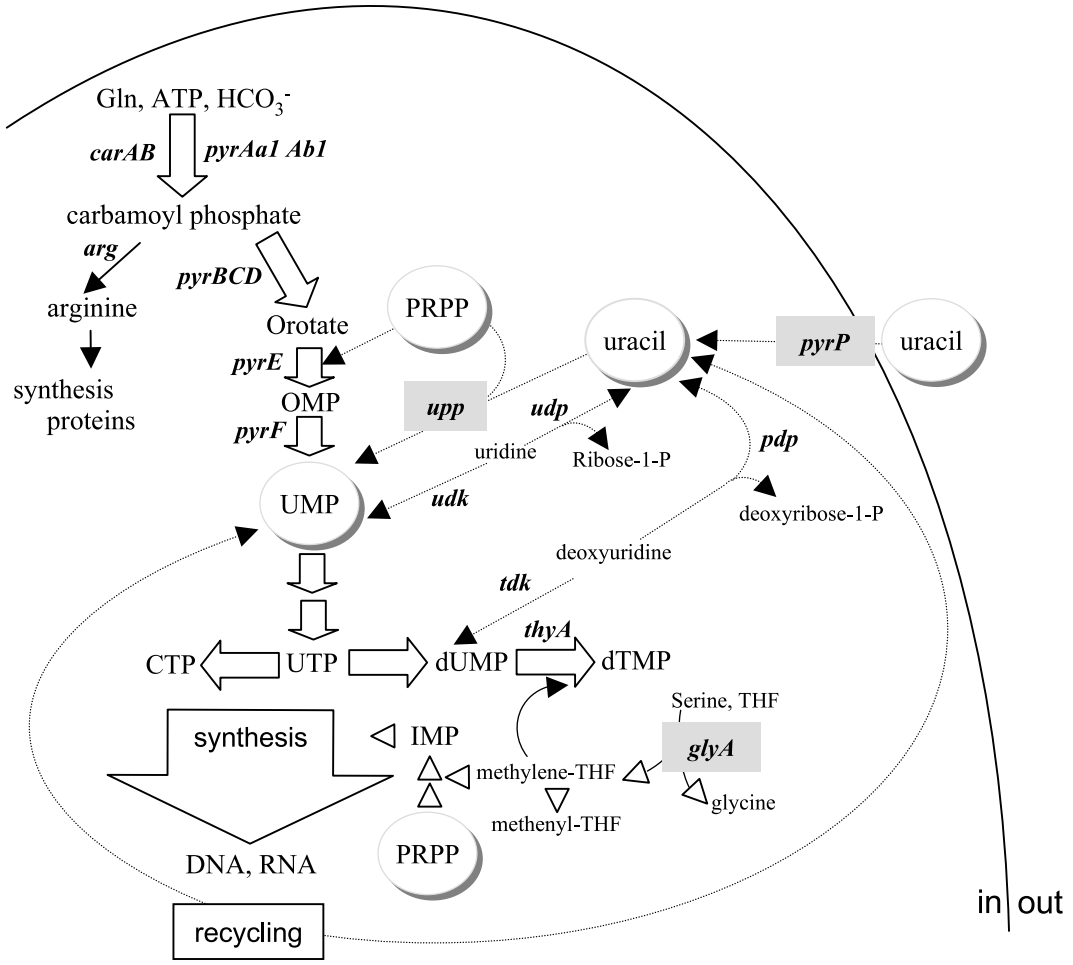


FIG. 1. Uracil salvage and pyrimidine biosynthetic pathways. Enzymes are identified by their corresponding gene designation for the uracil salvage pathway (thin arrows), de novo pyrimidine synthesis (thick arrows), and the IMP biosynthetic pathway (arrowheads), including steps involved in the incorporation of $C_1$ units from serine into THF. The enzymes catalyzing UMP synthesis are encoded by the *pyrR1-B-C-Aa1-Ab1-D-F-E* operon (9). Abbreviations for genes encoding enzymes are as follows: *glyA*, serine hydroxymethyltransferase (EC 2.1.2.1); *ndk*, nucleoside-diphospho kinase (EC 2.7.4.14); *udk*, uridine kinase (EC 2.7.1.48); *udp*, uridine phosphorylase (EC 2.4.2.3); *upp*, uracil phosphoribosyltransferase (EC 2.4.2.9); *pdp*, pyrimidine-nucleoside phosphorylase (EC 2.4.2.2); *pyrP*, uracil permease; *tdk*, thymidine kinase (EC:2.7.1.21); and *thyA*, thymidylate synthase (EC 2.1.1.45).

The transcription proceeds, and the structural genes are transcribed. Evidence that in *L. plantarum* the *pyr* operon is regulated by transcription attenuation in response to exogenous uracil has been obtained using transcription studies and intracellular pyrimidine triphosphate nucleoside pool size determination for wild-type and deregulated mutants (26): (i) mutations in conserved regions of *L. plantarum* PyrR1 and *B. subtilis* PyrR (flexible loop, phosphoribosyltransferase domain, and dimer loop/mRNA binding) suggested that these proteins are functionally similar; (ii) mutations of attenuation site no. 2 are located directly downstream of the *pyrR1* gene, such as in the consensus of the PyrR-binding hexaloop. Unlike *B. subtilis*, in *L. plantarum*, a second PyrR homolog encoded by the *pyrR2* gene shares 62% identity at the amino acid level with PyrR1. The *pyrR2* gene is not a member of the *pyr* operon, and its function has not been clarified yet (26).

Spontaneous uracil-deregulated mutants, including the *upp-pyrP* mutants characterized in this paper, were obtained in the genetic context of a strain impaired in the first step of UMP synthesis (26). This step leads to the formation of carbamoyl phosphate (CP) from glutamine, ATP, and inorganic carbon (carbon dioxide or bicarbonate) (Fig. 1). In *L. plantarum*, CP is synthesized by two carbamoyl phosphate synthases (CPS) (EC 6.3.5.5), the pyrimidine-repressed CPS-P encoded by the *pyrAa1-pyrAb1* genes present in the *pyr* operon and the arginine-repressed CPS-A encoded by the *carAB* operon (27). The presence of two functional CPS reflects the cells' need for CP in both the pyrimidine and the arginine biosynthetic pathways (Fig. 1). Deletion of both CPS conferred pyrimidine and arginine auxotrophy (27). Strain FB335 harbors a Δ*carAB* mutation so that CP synthesis relies solely on the pyrimidine-regulated CPS-P (27). In the presence of exogenous uracil believed to result in high UMP pools, strain FB335 growth was inhibited and the corresponding phenotype was designated uracil sensitive (Table 1). Uracil-resistant (UraR) spontaneous derivatives of the FB335 strain were isolated and partially characterized as previously described (26). Among the characterized genetic lesions that conferred the UraR phenotype, some mutations

TABLE 1. Characteristics of the *L. plantarum* subsp. *plantarum* strains

| Strain | Growth phenotype[b] | Pyrimidine excretion (μg/ml)[c] | 5FU MIC[d] | | Mutation(s)[a] |
|---|---|---|---|---|---|
| | | | With purines | Without purines | |
| CCM1904 | Prototroph | 0 | 0.03 | 0.0025 | Wild type |
| FB335 | UraS prototroph | 0 | 0.03 | 0.0025 | Δ*carAB* (27) |
| AE1023 | HCR | 0 | 0.03 | NT | Attenuation site at 2 mutated between *pyrR1* and *pyrB*, resulting in pyrimidine-independent low transcription of the *pyr* operon (26) |
| AE1026 | Prototroph | 4.3 | 0.03 | 0.0025 | PyrR1 D104Y (26) |
| U2 | HCR | 1.4 | 0.4 | NT | Δ*carAB* Δ*upp-pyrP*; chimeric Upp after residue S139; PyrP absent |
| U30 | HCR | 1.3 | 0.4 | 0.02 | Δ*carAB* Δ*upp-pyrP*; Upp and PyrP absent |
| U10 U35; U37 | HCR | 0.1 | 0.03 | NT | Δ*carAB* Δ*upp*; deletion of 7 residues (I12-I18) in Upp |
| U11 | HCR | 0.3 | 0.03 | NT | Δ*carAB* Δ*upp*; Upp C-terminal region truncation (S153-K209) |
| U20 | HCR | 2.0 | 0.03 | NT | Δ*carAB* Δ*upp*; Upp C-terminal region truncation (N154-K209) |
| U27 | HCR | 0.1 | 0.03 | 0.001 | Δ*carAB* Δ*upp*; Upp deletion (I55-K209) |
| U36 | HCR | 0.2 | 0.03 | NT | Δ*carAB upp*; Upp G81D due to mutation G783A |
| HN38 | HCR | 0.1 | 0.03 | 0.001 | Δ*carAB upp*::IS*Lpl1* (25) |
| U39 | HCR | 0.1 | 0.03 | NT | Δ*carAB upp*; Upp truncation of the C-terminal region from Q126 to K209 due to a point mutation (C662T) |

[a] Sequence data refer to EMBL accession number AJ012720 for the *upp-pyrP* locus.
[b] $CO_2$-dependent uracil and arginine nutritional needs were tested on the defined medium DLA that contains purines, no pyrimidines, and all amino acids but arginine. Prototrophs grew without arginine and uracil. UraS (uracil sensitive) prototroph growth was inhibited by uracil in DLA. HCR, high $CO_2$-requiring prototroph, which required exogenous arginine and uracil only at low carbon dioxide levels but not under carbon dioxide-enriched conditions. The HCR prototrophs are uracil resistant, as defined by their growth in the presence of uracil when carbon dioxide-enriched air was provided.
[c] μg of pyrimidine nucleotide/ml of full-grown culture supernatant.
[d] The MIC gives the minimal concentration in μg/ml of the toxic uracil analog 5FU, which inhibited the strain growth in the absence or presence of purines (adenine, guanine, hypoxanthine, and xanthine). NT, not tested.

invalidated PyrR1 or the transcription attenuator located between *pyrR1* and *pyrB* (26). In one UraR mutant (mutant HN38), the *upp* gene had an insertion of the mobile insertion sequence element IS*Lpl1* (25). The *pyrR1* mutants were prototrophs for both arginine and pyrimidines. Conversely, the *upp* mutant HN38 as well as the other uncharacterized UraR mutants were *h*igh $CO_2$-*r*equiring (HCR) prototrophs and required pyrimidines and arginine when grown in air but not in air enriched with carbon dioxide (26). These HCR mutants harbored wild-type *pyrR1* and *pyrR2* genes as well as wild-type *cis* regulatory regions of the *pyr* operon (localized before *pyrR1* and in the intergenic region between *pyrR1* and *pyrB*) and wild-type structural genes *pyrAa1-pyrAb1* of the CPS-P (26). In this paper, the uncharacterized deregulated mutants that displayed UraR and HCR phenotypes were shown to harbor genetic lesions in the *pyrP* and/or *upp* gene. Furthermore, the role of *upp* and *pyrP* in the pyrimidine salvage pathway in *L. plantarum*, their genetic organization, and their pyrimidine-dependent regulation were investigated.

## MATERIALS AND METHODS

**Lactobacilli and physiological tests.** All tested lactobacilli derive from the pyrimidine and arginine prototroph *L. plantarum* subsp. *plantarum* CCM 1904 (Table 1). Unless specified, cultures were performed at 30°C in air enriched with 4% $CO_2$ in a water-jacketed CH/P incubator (Forma Scientific). Pyrimidine and arginine nutritional requirements were tested in the presence of arginine (50 μg/ml) or uracil (50 μg/ml) at 30°C on DLA plates. The DLA medium contains purines: adenine (0.09 g/liter), guanine HCl (0.05 g/liter), hypoxanthine (0.03 g/liter), and xanthine (0.005 g/liter). The composition of the previously published DLA (6) was modified, with no deoxyguanosine added, Tween 80 replacing Tween 40 and oleic acid (1 g/liter). The DLP medium (26) was used for nucleotide pool size determination.

The MIC of the toxic uracil analog 5′-fluorouracil (5FU) was determined under two conditions: the presence and absence of purines. Cell suspensions (15 μl of $5.10^7$ cells/ml) were plated on DLA agar plates supplemented with arginine and increasing amounts of 5FU and incubated for 4 days. The amount of pyrimidines present in the culture supernatant of full-grown cells cultivated in DLA media supplemented with 50 μg/ml of arginine was quantified with a bioassay using the uracil auxotroph strain HN217 (26).

**DNA techniques.** The *upp* and *pyrP* genes were sequenced from strain CCM 1904 on two overlapping PCR-amplified fragments, using different primer sets (Table 2). The PCRs were performed as previously described (26).

**Transcription studies.** RNAs were extracted from strains U27, FB335, and CCM 1904, which displayed similar growth rates (data not shown) in mid-exponential growth phase (an optical density at 600 nm of 0.4), using TRIzol reagent (Invitrogen) as previously described (24). Contaminant DNA was removed by incubating the RNA extracts for 20 min at 37°C in the presence of DNase I (Amersham Biosciences), which was subsequently heat inactivated. Reverse transcriptase (RT) PCR was performed using the SuperScript one-step RT-PCR with a platinum *Taq* kit (Invitrogen) under the conditions previously described (24). Regulation of transcription was determined using Northern slot blot analysis. The *upp* and *pyrP* probes were PCR amplified (Table 2) and digoxigenin labeled, and the concentrations were estimated using the labeled DNA control from the digoxigenin DNA labeling and detection kit (Roche). For each probe, the optimal amount of RNA to be used for quantification was tested in the range of 0.1 to 20 μg of total RNA and was found to be different from those of the *upp* (2 μg), *pyrP* (20 μg), *pyrAb1* (2 μg), and *rrn* (0.1 μg) transcript detections. Conditions of Northern hybridization and detection of the DNA-RNA hybrids with the alkaline phosphatase chemiluminescent substrate CDP-Star (Roche) were previously specified (24). At least two independent assays were performed for each tested condition. The background level was subtracted from the measured signal quantified with Quantity One software (Bio-Rad). For each probe, the level of expression was estimated by dividing the measured probe signal by the measured *rrn* signal.

**Cloning of *L. plantarum upp* gene in *E. coli*.** The *upp* gene was PCR amplified from the *L. plantarum* wild-type strain CCM 1904 with primer set LPupp-f/LPupp-r (Table 2), using the Promega *Pfu Taq* polymerase and cycles of denaturation at 94°C for 45 s, hybridization at 52°C for 45 s, and elongation at 72°C for 2 min 30 s. After 35 cycles, a postelongation at 72°C for 30 min was performed. The resulting 0.77-kb fragment was ligated in the cloning vector pUC18 (4) after digestion with the restriction enzymes BamHI and HindIII, respectively, present at unique sites in primers LPupp-f and LPupp-r. The ligation mixture was electroporated into *E. coli* TG2, and white transformants were selected on LB plates containing X-Gal (5-bromo-4-chloro-3-indolyl-β-D-galactopyranoside) (32 μg/ml) and ampicillin (50 μg/ml). One of these clones harbored plasmid pLPupp, whose insert contained the *L. plantarum upp* gene wild-type sequence (data not shown) expressed from the vector's promoter. *L. plantarum upp* function has been tested by complementation in the *E. coli*-deficient *upp udp pyrF* strain

TABLE 2. Primer list

| Genetic locus (EMBL database accession no.) and use(s)[a] | PCR product size (kb) | Primer name | Primer sequence (5′→3′)[b] |
|---|---|---|---|
| *lp_2376-glyA-upp-pyrP* (AL935263) | | | |
| RT-PCR primer set a | 0.3 | LPpyrP-g4 | AATCATTCACAAAAAGGGGTGCG (F) |
| | | LPpyrP-d2 | TCATCAGAGACTGCATCACAACG (R) |
| RT-PCR primer set b | 2.0 | LPupp-SG | GTTTGAGGTTTTGGATCATCCGC (F) |
| RT-PCR primer set c | 1.3 | orfph-d2 | AATTAGATTGTTGTACGTCAGCC (R) |
| RT-PCR primer set d | 0.4 | LPupp-H1 | TATCCATCGCCATGATGGCTGAACC (R) |
| RT-PCR primer set e | 0.7 | glyc-g1 | CGGTCAACAAAGAAGCGATTCCG (F) |
| RT-PCR primer set f | 2.0 | Lp2375f | TGGGCGTTATGGCAACAGATG (F) |
| RT-PCR primer set g | 0.5 | Lp2376r | CAGAGTATTTATTGGTCAGCA (R) |
| *pyrP* probe (LPpyrP-g4/LPpyrP-d1) | 0.6 | LPpyrP-d1 | CGGCAATGATATACCCACAGACG (R) |
| *upp* amplification and sequencing | 2.4 | LPupp-E2 | ATGATTCCGGCAGCTAAAGTTGG (F) |
| | | orfph-g1 | CGAATGGCTGACGAAGATGTACC (F) |
| *upp* cloning | 0.8 | LPupp-f | CTATCGGATCCACTAAGGAGTGTGCGTAGC (F) |
| | | LPupp-r | CGATATTAGTAGGCGTAAGACACTTCGAAGTAT (R) |
| *pyrP* amplification and sequencing | 1.9 | orfph-g3 | GGGTGAGAAAGTCACATTATTTC (F) |
| | | LPatp-d3 | CGTCAGTCCAAGGAATTTGACTG (R) |
| | | LPpyrp-g3 | CTTCAAGTGGGATGCGAATTCTG (F) |
| *rrn* (AL935263) | | | |
| RT-PCR and *rrn* probe | 0.4 | 907r | CCGTCAATTCCTTTGAGTTT (F) |
| | | 530f | GTGCCAGCAGCCGCGG (F) |
| *pyrAb1* (X99978) | | | |
| RT-PCR and *pyrAb1* probe | 0.4 | N58 | CAGCTTCTGGTATTGCGC (F) |
| | | 2005 | ATCTTCAAAGCAGCATCCCG (R) |

[a] Primer sets are indicated in Fig. 4A. The *upp* probe was obtained with primers LPupp-H1/LPupp-SG.
[b] F, forward primer; R, reverse primer.

BM604 (2) on minimal medium M9 supplied with either uracil or uridine at 10 or 20 μg/ml, respectively.

**Uracil transport assays.** Exponentially grown cells (an optical density at 450 nm of 0.5) in DLA medium were transferred to an Eppendorf tube containing $^{14}$C-labeled uracil at a specific activity of 52 mCi/mmol. Samples were taken after 15, 30, 45, and 60 seconds using uracil concentrations ranging from 5 to 0.2 μM. The cells were trapped by filtration through a 0.22-μm filter, and the remaining medium was removed by two washes with 5 ml 0.9% NaCl and 100 μM uracil at room temperature. The radioactivity on the filters was determined in a scintillation counter. A filter with a medium sample was included in order to determine the specific activity in the individual experiments. The uptake was linear for up to 60 seconds, even at 0.5 μM. Consequently, an incubation time of 30 seconds was used to determine the kinetic constants. The classical Michaelis-Menten constants $K_m$ and $V_{max}$ were calculated by plotting the data in a double-reciprocal plot. Assuming that an optical density of 1 at 450 nm corresponds to $3.10^8$ cells/ml, the uptake rate was determined in uracil molecules per second per cell.

**Determination of the nucleotide pools.** Intracellular nucleotide pool quantification in *L. plantarum* has been previously described (26).

## RESULTS

Mutations that may alter preformed uracil utilization were searched in 10 pyrimidine-deregulated derivatives of strain FB335. The phenotypes of these mutants were previously characterized as UraR, high $CO_2$-requiring prototrophy, and excretion of low amounts of preformed pyrimidine bases and nucleosides (26). The sequence of the *upp-pyrP* locus in the mutants was compared to that of the wild type. All mutants harbored lesions in *upp* (Table 1 and Fig. 2). In addition to the *upp* mutation, the adjacent *pyrP* gene was also mutated in strains U2 and U30. The genetic lesions were point mutations in two strains (U36 and U39), deletions ranging from 1 to 2,400 nucleotides in seven strains (U2, U10, U11, U20, U30, U35, and U37), insertion of 22 nucleotides in strain U27, and insertion of IS*Lpl1* in the previously described strain HN38 (25). Six mutants (U30, U2, U27, U39, U11, and U20) had major truncations (25% to 100%) of the *upp* open reading frame (Fig. 2). The same 21-nucleotide (nt)-long deletion was found in three mutants (U10, U35, and U37) that led to the loss of the seven residues in the N-terminal part of the UPRT.

***L. plantarum upp* gene codes for a UPRT.** To verify that the *upp* gene was coding for a functional UPRT, the ability of the *L. plantarum upp* gene to complement a deficient *upp E. coli* mutant was assessed. An *L. plantarum upp* gene present in plasmid pLPupp was introduced by transformation into *E. coli* strain BM604. Strain BM604 (*upp*, *pyrF*) requires uridine in order to grow and has a pyrimidine requirement which uracil is unable to satisfy (2). Transformants were tested on minimal medium M9 in the presence of either uracil or uridine. Only transformants harboring plasmid pLPupp grew in the presence of uracil (data not shown). Thus, the *L. plantarum upp* gene codes for a UPRT enzyme that is functional in the heterologous *E. coli* genetic background.

**Kinetic constants of *L. plantarum* uracil uptake transporter PyrP.** Increased resistance to the toxic uracil analog 5FU was seen only when both *pyrP* and *upp* genes were mutated as found in strains U2 and U30 (Table 1). The 5FU resistance could be explained if *pyrP* would encode a uracil transporter. To investigate whether *pyrP* encodes a uracil transporter, the uptake of $^{14}$C-labeled uracil was measured in strains U2 (Δ*pyrP* Δ*upp*), U27 (Δ*upp*), and FB335 (wild-type *pyrP* and wild-type *upp*). The U2 mutant was no longer able to transport uracil across the membrane, whereas uracil was transported across the membrane in strain U27 (Fig. 3) and in the strain FB335 (data not shown). Thus, under the tested conditions, *pyrP* was the only high-affinity uracil transporter in *L. plantarum*. The kinetic properties of uracil uptake were determined in genetic backgrounds that minimized rapid uracil utilization after cell entry. Since at least 97% of the incoming uracil was metabolized by the UPRT encoded by *upp* in *L. lactis*

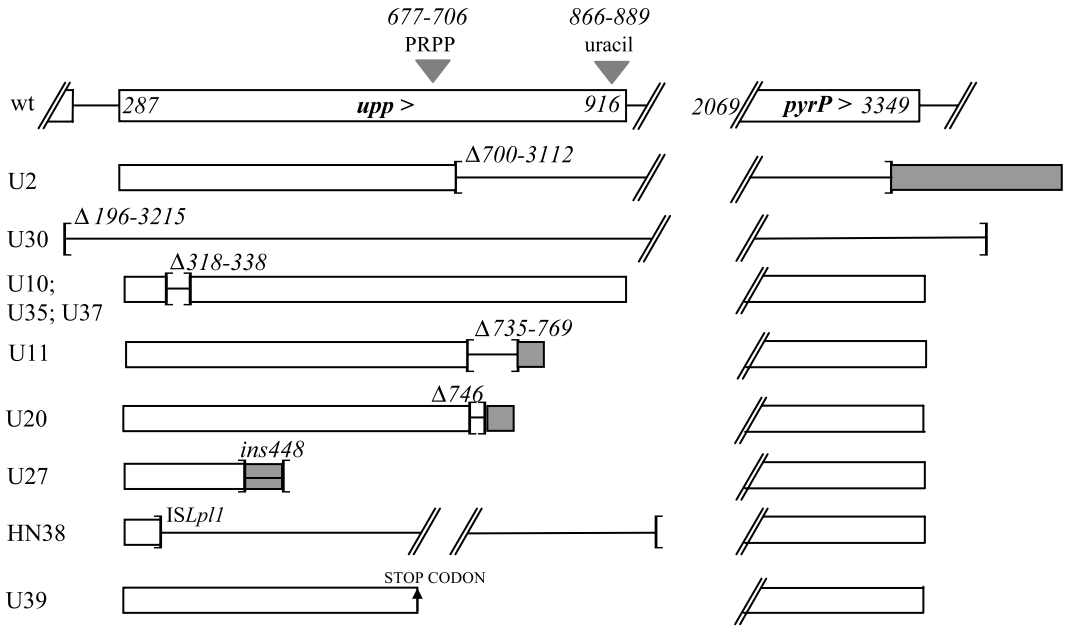


FIG. 2. Analysis of the *upp* and *pyrP* mutations found in spontaneous uracil-resistant clones. Genes are schematized as white rectangles when the resulting protein is wild type (wt) or as gray rectangles when mutations led to chimeric proteins. Strain names are indicated on the left. PyrP was inactivated only in strains U30 and U2. Insertion and deletion events delineated by brackets are oriented outwards and inwards, respectively. In strain HN38, the mobile insertion sequence IS*Lpl1* inactivated *upp* (25). In mutant U27, the sequence 5′-TATGCCGTTGAAGGACATTG AG-3′ was inserted at nucleotide 448. Numbers refer to nucleotide positions in the EMBL database sequence accession no. AJ012720. The PRPP- and uracil-binding sites were determined using UPRT sequence alignments as determined in reference 29.

(17) and since UPRT is the key enzyme in the preformed uracil utilization pathway in microorganisms (22), strain U27 was used to determine the kinetic constants of uracil uptake in *L. plantarum*. The $K_m$ value for uracil was 0.7 ± 0.1 μM; $V_{max}$ was 3.5 × $10^3$ ± 0.6 × $10^3$ molecules per second per cell.

**The *pyrP* gene and the *upp* gene are not cotranscribed.** The four genes *lp_2376*, *glyA*, *upp*, and *pyrP* were contiguous on the *L. plantarum* genome and oriented in the same direction. The *upp* and *pyrP* 1,257-base-pair intergenic region was found to be well conserved between strains CCM 1904 and WCFS1 (less than 0.8% divergence), and no protein coding sequence was detectable in silico. To test whether these genes were cotranscribed, reverse transcriptions coupled with PCR amplifications were performed on mRNA extracts with different primer sets (Fig. 4A) and included the following controls. The specificity of hybridization of the primer sets was verified in classical PCR amplification using DNA matrices (Fig. 4B, lanes with an asterisk). The absence of contaminant DNA templates was confirmed (Fig. 4B, lanes 9, 10, 12, and 13). Transcription of genes *pyrP* and *upp* was identified using primer sets a and d, respectively (Fig. 4B, lanes 6 and 15). The *upp-pyrP* cotranscription was assessed with primer set b (Fig. 4B, lanes 9 and 10). Transcription from *upp* into the intergenic region was tested with primer set c (Fig. 4B, lanes 12 and 13). No RT-PCR products were obtained with increasing amounts (30 ng to 200 ng) of mRNA extracted from cells grown with or without uracil, indicating the absence of *upp-pyrP* cotranscription. Transcription arrest after *upp* and *pyrP* may occur at distinct predicted rho-independent terminators, located 11 nucleotides after the *upp* stop codon (nt 928 to 969; $\Delta G$ of −20.7 kcal · $mol^{-1}$) and 50 nucleotides downstream of the *pyrP* stop codon (nt 3399 to 3440; $\Delta G$ of −14.1 kcal · $mol^{-1}$) (database accession no. AJ012720).

Cotranscription of the *lp_2376-glyA-upp* genes was tested by RT-PCR using three primer sets, g, f, and e (Fig. 4B, lanes 20, 19, and 17, respectively). The sizes of the PCR products support the conclusion that the three genes are transcribed as a polycistronic message of approximately 3 kb. A sequence (TT GACA < 17 bp > aATAAa) with only two mismatches (shown in lowercase) compared to the *L. plantarum* consensus promoter sequence (TTGACA < 17 bp > TATAAT) was found 56 bp upstream of the *lp_2376* initiation codon. From these transcription studies, we concluded that *lp_2376-glyA-upp* formed a separate transcriptional unit not including *pyrP*.

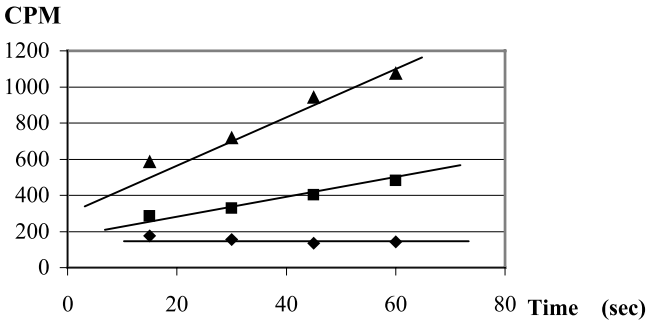


FIG. 3. Uracil transport in the *pyrP* strain. Radioactively labeled uracil was added at 0.5 μM to *L. plantarum* U2 (*upp*, *pyrP*) (diamonds), 0.5 μM to U27 (*upp*) (squares), and 1.0 μM to U27 (triangles). Samples were filtered at 15-second intervals, and the radioactivity retained by the cells was measured and plotted against the incubation time.

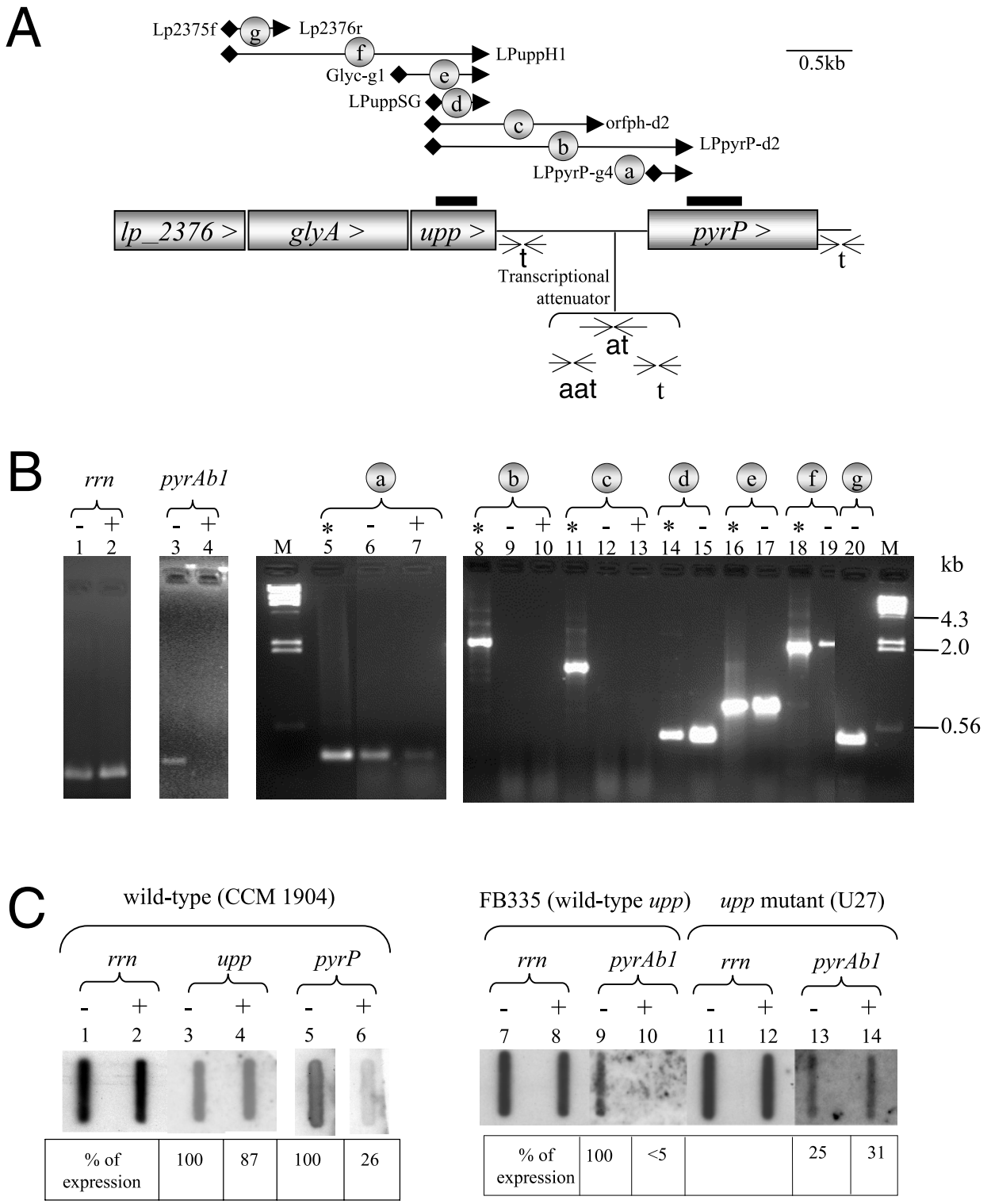


FIG. 4. Results of transcriptional studies of the *upp-pyrP* locus in *L. plantarum*. (A) Gene organization and transcription terminator localization. The orientation and the name of the genes are indicated in rectangles. Sequences involved in RNA hairpin structures are schematized with facing arrows and labeled t (*t*erminator), at (*a*nti*t*erminator), or aat (*a*nti-*a*nti*t*erminator). In circles, primer sets are named from a to g. Filled diamonds represent forward primers, and filled arrowheads represent reverse primers. Thick black lines delineate DNA probes used in Northern slot blot analysis. (B) Results of reverse transcriptase coupled with PCR amplification. The sizes of the expected bands were controlled by PCR amplification in the presence of CCM 1904 genomic DNA (lanes marked with an asterisk), and band sizes were estimated using DNA molecular marker bands (lane M). RNAs were extracted from cells grown with (+) or without (−) 50 μg/ml of uracil in defined DLA medium (for the presented experiment, cells were grown in aerobiosis but similar amplification patterns were obtained with cells grown in air enriched with 4% $CO_2$). RT-PCR was performed with different RNA amounts: 20 ng for the 16S *rrn* gene (lanes 1 and 2) and the *pyrAb1* gene (lanes 3 and 4),

**Pyrimidine repression of the *pyrP* gene and pyrimidine-independent transcription of the *upp* gene.** Pyrimidine-dependent expression of the *pyrP* and *upp* genes was assessed by RT-PCR and Northern slot blot analysis on mRNA extracted from cells grown with or without uracil. Two controls were performed: (i) pyrimidine repression was checked with a previously described *pyrAb1*-specific probe (Fig. 4C, lanes 9 and 10) (26), and (ii) pyrimidine-independent transcription of the *rrn* locus enabled the quantification of the relative mRNA extracted in the absence and presence of uracil (Fig. 4B [lanes 1 and 2] and C). When *pyrP* mRNA presence was assessed with primer set a (Fig. 4A), less RT-PCR product was obtained in mRNA extracted from cells grown in the presence of uracil than in mRNA extracted from cells grown without it (Fig. 4B, compare lanes 7 and 6). The pyrimidine-dependent repression of the *pyrP* gene was confirmed by Northern slot blot analysis with a *pyrP* probe. Only one quarter of the relative amounts of *pyrP* mRNA was measured in RNA extracts of cells cultivated in the presence of uracil compared to those of cells cultivated in the absence of uracil (Fig. 4C, compare lanes 6 and 5). Unlike with the *pyrP* probe, the relative amounts of *upp* mRNA detected with a specific *upp* probe were similar under both tested conditions (Fig. 4C, lanes 3 and 4). Thus, transcription of *pyrP* was regulated in response to exogenous uracil, whereas *upp* transcription was not.

**Mutation in *upp* altered the uracil-dependent regulation of the biosynthetic *pyr* operon.** Unlike the uracil-sensitive parental strain FB335, whose growth depended on expression of the pyrimidine-repressed carbamoyl phosphate synthase (CPS-P), its *upp* derivatives were resistant to exogenous uracil. This ability to grow in the presence of uracil suggested the loss of pyrimidine-dependent regulation of the CPS-P-encoding genes *pyrAa1-pyrAb1*. Thus, the transcription levels of *pyrAb1* were compared in strains harboring a wild-type and an inactive *upp* gene (Fig. 4C, compare lanes 7 to 10 with lanes 11 to 14). In the presence of uracil, significantly higher amounts of *pyrAb1* mRNA were detected in the *upp* mutant U27 than in strain FB335 that harbored the wild-type *upp* gene (Fig. 4C, compare lanes 14 and 10). Moreover, in the absence of uracil, the amount of *pyrAb1* mRNA was four times less in the *upp* mutant than in the wild-type strain (Fig. 4C, compare lanes 13 and 9). We concluded that in *upp* mutants, the *pyr* operon that includes the *pyrAa1Ab1* genes was constitutively expressed whether or not exogenous uracil was added to the media, which explains why the *upp* mutants were no longer sensitive to exogenous uracil.

To investigate whether the *upp* mutation conferred dramatic changes in the UTP level, the nucleotide pool sizes were measured in strain U27. A mutation in the *upp* gene did not affect nucleotide triphosphate pool sizes, as strain U27 had the same pool size as the parental strain FB335 (data not shown).

## DISCUSSION

The roles of *pyrP* and *upp* in the *L. plantarum* uracil salvage pathway were studied by genetic and physiological analysis. Allelic mutations in the *pyrP* gene conferred increased resistance to the toxic uracil analogue 5FU (Table 1) and impaired transport of radioactively labeled uracil when present in the micromolar scale (Fig. 3). Thus, the *pyrP* gene encodes a high-affinity uracil uptake facilitator. The *upp* gene codes for a functional UPRT since it complemented an *E. coli upp* mutant. UPRTs are members of the phosphoribosyl transferase family (Pfam accession number PF00156), defined by their protein fold and by a short sequence motif termed the "PRPP-binding site." This motif was affected in mutant U36 by a G81D missense mutation. *L. plantarum upp* mutants excreted low amounts of uracil (0.1 to 0.5 μg/ml; one unexplained exception was mutant U20 that excreted 2.0 μg uracil per ml). In *upp* mutants of other microorganisms, such as *E. coli* (12) and *L. lactis* (17), a small increase in pyrimidine excretion has also been observed. Pyrimidine excretion can be explained by the inability of *L. plantarum* mutants to recover uracil arising from intracellular nucleotide turnover. We concluded that UPRT activity is required for optimal pyrimidine turnover in *L. plantarum*.

**5-Fluorouracil metabolism in *L. plantarum*.** 5FU is an analog of uracil, which is cytotoxic only after being converted by the pyrimidine salvage pathway enzymes to the nucleotide level. The most toxic metabolite formed inside the cell is 5-fluorodeoxyuridine monophosphate, which covalently binds to thymidylate synthase (*thyA*), the enzyme catalyzing the formation of dTMP from dUMP. Most microorganisms with impaired UPRT activity have increased 5FU resistance (22). However, in *L. plantarum*, the *upp* mutation had no effect on 5FU resistance in the absence of purine bases (Table 1). This is consistent with the observation made with *L. lactis*, where UPRT deficiency resulted only in a small effect on 5FU sensitivity. It was shown to be due to a direct conversion of 5FU to 5-fluorodeoxyuridine monophosphate through the action of pyrimidine phosphorylase utilizing deoxyribose-5-phosphate and thymidine kinase (17). A similar observation was made with *B. subtilis* (16). In media with purine bases, only the *upp pyrP* strain was more resistant towards 5FU than the parental strain. This unexpected observation could be explained by the fact that 5FU was taken up by the cell even when the uracil transporter (*pyrP*) was mutated, and candidates for facilitating this uptake could be purine base transporters. In the presence of exogenous purine bases, 5FU was significantly reduced due to the function of purine bases as competitive inhibitors of 5FU transport. This idea is supported by the finding that in the absence of purine bases, the *pyrP* mutant was 20 times more sensitive to 5FU (Table 1).

75 ng for the *pyrP* gene (lanes 6 and 7), the *upp* gene (lane 15), and the *lp_2376-glyA-upp* gene cluster (lanes 17, 19, and 20), and 200 ng for the intergenic *upp-pyrP* region (lanes 9 to 10 and 12 to 13). (C) Northern slot blots with probes specific to the *rrn* gene, the *pyrP* gene, the *upp* gene, and the *pyrAb1* gene in the parental strain harboring a wild-type *upp* gene (lanes 1 to 10) and in its *upp* derivative strain U27 (lanes 11 to 14). The percentage of expression was calculated with two independent experiments. The relative amount of mRNA (signal measured with the test probe divided by the signal detected with the *rrn* probe) of the mutant was compared to the relative amount obtained with the wild type grown without uracil (100%).

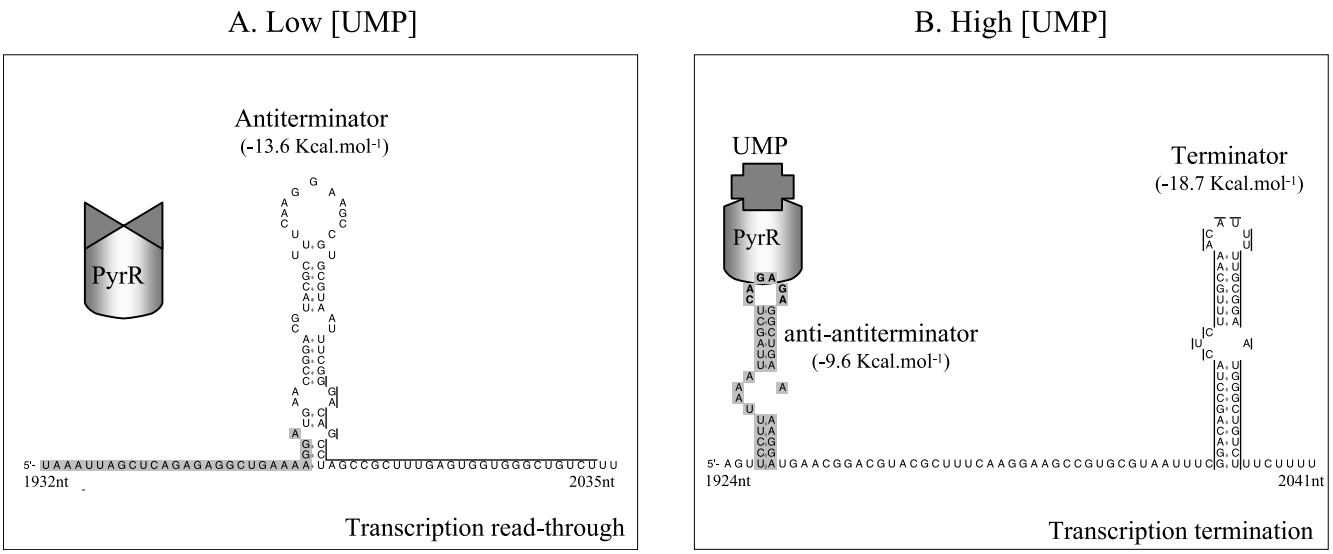


FIG. 5. Model of pyrimidine-dependent transcription attenuation. The transcription attenuation site sequence of the *pyrP* gene is shown (nucleotides 1924 to 2033 in EMBL database sequence accession no. AJ012720). (A) When the PyrR regulator remains unbound, the formation of the RNA loop antiterminator allows for the transcription of the downstream gene. (B) When the PyrR-UMP complex is bound to the hexaloop CAGAGA (in bold) at the tip of the anti-antiterminator hairpin, the terminator RNA loop can form and transcription stops before the downstream *pyr* gene. The $\Delta G$ values of the proposed RNA loops are indicated in parentheses.

**Model of *pyrP* pyrimidine-dependent regulation by transcription attenuation.** When wild-type *L. plantarum* was grown in the presence of uracil, *pyrP* transcription was reduced fourfold (Fig. 4B and C). PyrR-mediated transcription attenuation of the *pyrP* genes has been documented in other bacteria, such as *B. subtilis* (32), *Bacillus caldolyticus* (11), *Enterococcus faecalis* (10), and *L. lactis* (18). In *L. plantarum*, the *pyrP* leader mRNA harbors a good predicted transcription attenuation site (Fig. 5). The tip of the predicted anti-antiterminator stem is formed by a hexaloop CAGAGA identical to the proposed PyrR binding site (5, 26). The presence of the predicted transcription attenuation site and the measured decrease in *pyrP* transcription in response to exogenous uracil suggest that the *pyrP* gene, like the *pyr* operon, is regulated by PyrR-mediated transcription attenuation in *L. plantarum*.

**Reduced CPS-P expression triggers $CO_2$ nutritional needs.** The *upp* mutants displayed a high $CO_2$ requirement for arginine and pyrimidine prototrophy. The HCR phenotype has previously been proposed to result from low intracellular CP pools under low inorganic carbon growth conditions, since $CO_2$ is a substrate required in CP synthesis and since CP is a precursor in arginine and pyrimidine synthesis (Fig. 1). Low CP pools could be due to low CPS activity and/or to reduced amounts of CPS (7). CPS-P is the major source of CP for *L. plantarum* grown at low $CO_2$ levels and can provide enough CP for both biosynthetic pathways (27). Mutant AE1023 was an HCR prototroph with low CPS-P expression due to constitutive low transcription of the *pyr* operon (F. Arsène-Ploetze and F. Bringel, unpublished data) (26). The *upp* mutants displayed the HCR phenotype and lowered CPS-P expression in the absence of uracil (Fig. 4C). These observations in different genetic contexts (AE1023 and *upp* mutants) raise the question of whether low CPS-P expression implies higher $CO_2$ nutritional needs under conditions where arginine and pyrimidines are not provided. Previous studies have suggested that intracellular $CO_2$ levels may be naturally low in *L. plantarum* grown under laboratory conditions since the two $CO_2$-producing steps of the Krebs cycle (isocitrate dehydrogenase and 2-oxoglutarate dehydrogenase) are inoperative in *L. plantarum* (20). Low $CO_2$ levels would be a limiting factor of CPS-P activity in *L. plantarum* grown without $CO_2$ enrichment. In the wild-type strain, the CPS-P amount is sufficient to compensate for $CO_2$ substrate shortage. However, in the case of reduced CPS expression (as in AE1023 and *upp* mutants) and substrate shortage (as when grown in ordinary air), CP synthesis would be too low to sustain arginine and pyrimidine prototrophy. By increasing the $CO_2$ supply, CPS-P activity would increase, enough CP would be synthesized, and arginine and pyrimidine prototrophy would be restored in the mutants. We concluded that reduced CPS-P expression in the absence of uracil in *L. plantarum* explains its higher $CO_2$ nutritional needs.

**Can the UMP pools explain deregulated expression of the *pyr* operon in the *upp* mutants?** Compared to a strain harboring wild-type *upp*, in the *upp* mutant, transcription of the *pyr* operon was reduced fourfold when uracil was absent (Fig. 4C, compare lanes 9 and 13). Therefore, a functional *upp* is required for maximal expression in the absence of exogenous uracil. On the other hand, in the presence of uracil, higher expression of the *pyr* operon was observed in the *upp* mutant than in the wild type, where no expression was detected (Fig. 4C, compare lanes 14 and 10). Thus, a functional *upp* gene would be required in pyrimidine-dependent repression of the *pyr* operon. Inactivation of the *upp* gene resulted in the loss of the pyrimidine-dependent regulation so that the *pyr* operon expression levels were similar whether or not exogenous uracil was present (Fig. 4C, compare lanes 13 and 14). The *L. plantarum* repressor PyrR1 mediates pyrimidine-dependent transcription attenuation of the *pyr* operon (26). Mutations in the

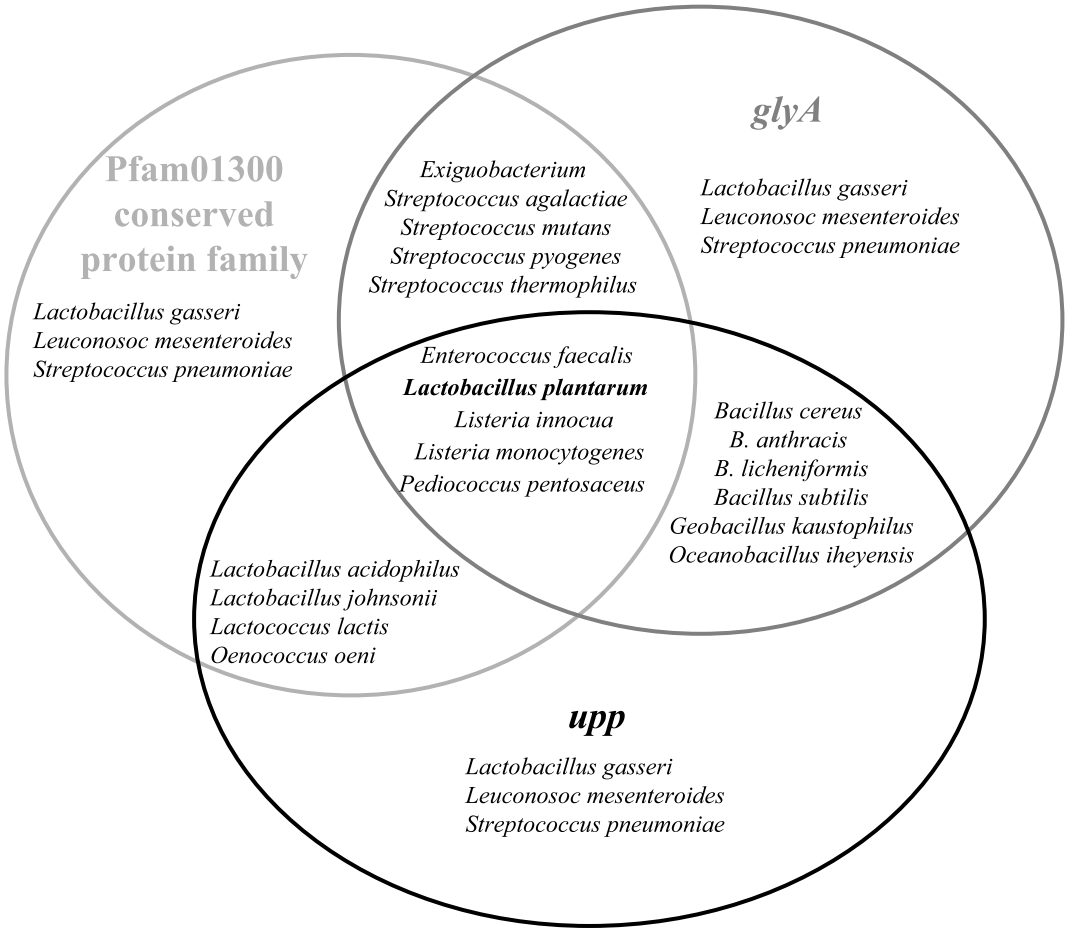


FIG. 6. Gene linkage of *lp_2376-glyA-upp* genes in gram-positive bacteria. Black, gray, and light-gray circles refer to the distributions of the *upp*, *glyA*, and *lp_2376* genes, respectively. Names of bacteria in which a genetic linkage of two genes was observed (cluster) are found in the circle intersection. In the intersection of the three circles are bacteria names with linked *lp_2376-glyA-upp* genes.

UMP/PRPP coregulator binding sites of *L. plantarum* PyrR1 reduced its repressor function. So, as demonstrated for *B. subtilis* PyrR (31), the ratio of UMP to PRPP is likely to regulate *L. plantarum* PyrR1 activity. This would imply that in the *upp* mutants, deregulation of the *pyr* operon may result from different PyrR1 expression levels or different UMP/PRPP ratios compared to those of the wild-type strain. Concerning the UMP/PRPP ratios, at least in the absence of uracil, the intracellular PRPP levels were similar in the wild-type and *upp* strains (data not shown), suggesting that the PRPP pool was not responsible for the observed deregulation. Since we have demonstrated that *upp* mutants were impaired in exogenous uracil assimilation and recycling of uracil derived from RNA degradation, the change in UMP concentration would infer deregulation. As a conclusion, we propose that the deregulation of the *pyr* operon observed in the *upp* strains would be the result of altered control of the activity or expression of the repressor PyrR1 by impaired intracellular pools of its effectors. Since PyrR1 was demonstrated not to be entirely responsible for *pyr* operon repression (26), another mechanism may also be involved.

***lp_2376-glyA-upp* operon.** The *upp* gene is cotranscribed with two upstream genes: *lp_2376* and *glyA*. Gene *lp_2376* codes for a putative 334-amino-acid-long protein that belongs to a conserved protein family with the C-terminal conserved domain (154 residues) of the *sua5-yciO-yrdC* domain (Pfam01300, Swiss-Prot/TrEMBL database), whose members can be found in prokaryotes and eucaryotes. Suggested members of this family are YciO and HypF (*E. coli*), YwlC (*B. subtilis*), Sua5 (*Saccharomyces cerevisiae*), and YrdC (*Drosophila melanogaster* and humans). Sua5 has been proposed to be involved in the reinitiation of translation (21). The C-terminal domain of *E. coli* YrdC has been shown to preferentially bind to double-stranded RNA and has been proposed as a putative ribosome maturation factor (14, 30). The implication of *lp_2376* in translation has not been tested so far in *L. plantarum*.

To evaluate whether other gram-positive bacteria might also harbor such an operon, the genetic linkage and respective gene orientation of the three genes were analyzed in sequenced genomes (Fig. 6). The gene order *lp_2376-glyA-upp* found in *L. plantarum* was conserved in the two *Listeria* species, *E. faecalis*, and *Pediococcus pentosaceus*. In other gram-positive bacteria, only two of the three genes were contiguous or interspaced by fewer than two genes. The genes were always oriented in the same direction within a gene cluster. This genetic linkage was not found in *Lactobacillus gasseri*, *Leuconostoc mesenteroides*,

and *Streptococcus pneumoniae*. The fact that at least two genes were genetically linked in 16 gram-positive bacteria (Fig. 6) prompted us to search for metabolic links between them. Whereas the function of *lp_2376* is unknown, the *glyA* gene is well characterized. The corresponding enzyme is responsible for the incorporation of $C_1$ units from serine into tetrahydrofolate (THF) (Fig. 1). The $C_1$ units of formyl-THF and methenyl-THF are the $C_1$ donors in pantothenate (vitamin $B_5$) biosynthesis in reactions catalyzed by PanB (EC 2.1.2.11), as well as in the purine biosynthetic pathway in reactions catalyzed by the PurN and PurH transformylases. Furthermore, one-carbon units are also required for the synthesis of the unique nucleotide component of DNA, thymidylate. The conversion of dUMP to thymidylate involves a methylation at C-5 of the uracil ring, with one carbon unit donated by methylene-THF (19). Thus, a gene involved in pyrimidine metabolism is linked and coexpressed with a gene involved in purine metabolism. The *glyA* gene is a member of the PurR regulon and is induced under general purine starvation in *L. lactis* (3) and *B. subtilis* (28). PRPP is the effector molecule in PurR-mediated regulation and functions as an inducer of *pur* genes by binding to the PurR protein. In *B. subtilis*, PurR acts as a repressor, preventing transcription initiation by binding in the promoter region. PRPP induces transcription since the PRPP-PurR complex no longer binds to the DNA (8). In *L. lactis*, the PRPP-PurR complex is an activator of transcription (15).

Under conditions of high intracellular uracil and PRPP pools, UPRT would catalyze UMP synthesis from uracil, while GlyA would provide $C_1$ units for PRPP-PurR-induced IMP synthesis and thymidylate synthesis. Thus, under conditions of high PRPP and low UMP pools, GlyA and UPRT would be coexpressed and would contribute to balance purine and pyrimidine metabolisms in these microorganisms. This model will be tested by proteomic and transcriptional studies of *L. plantarum* under conditions of purine depletion or deregulation.

## REFERENCES


1. **Andersen, P. S., D. Frees, R. Fast, and B. Mygind.** 1995. Uracil uptake in *Escherichia coli* K-12: isolation of *uraA* mutants and cloning of the gene. J. Bacteriol. **77:**2008–2013.
2. **Andersen, P. S., J. M. Smith, and B. Mygind.** 1992. Characterization of the *upp* gene encoding uracil phosphoribosyltransferase of *Escherichia coli* K12. Eur. J. Biochem. **204:**51–56.
3. **Beyer, N. H., P. Roepstorff, K. Hammer, and M. Kilstrup.** 2003. Proteome analysis of the purine stimulon from *Lactococcus lactis*. Proteomics **3:**786–797.
4. **Bolivar, F., R. L. Rodriguez, M. C. Betlach, and H. W. Boyer.** 1977. Construction and characterization of new cloning vehicles. I. Ampicillin-resistant derivatives of the plasmid pMB9. Gene **2:**75–93.
5. **Bonner, E. R., J. N. D'Elia, B. K. Billips, and R. L. Switzer.** 2001. Molecular recognition of *pyr* mRNA by the *Bacillus subtilis* attenuation regulatory protein PyrR. Nucleic Acids Res. **29:**4851–4865.
6. **Bringel, F., L. Frey, S. Boivin, and J. C. Hubert.** 1997. Arginine biosynthesis and regulation in *Lactobacillus plantarum*: the *carA* gene and the *argCJBDF* cluster are divergently transcribed. J. Bacteriol. **179:**2697–2706.
7. **Bringel, F., and J.-C. Hubert.** 2003. Extent of genetic lesions of the arginine and pyrimidine biosynthetic pathways in *Lactobacillus plantarum*, *L. paraplantarum*, *L. pentosus*, and *L. casei*: prevalence of $CO_2$-dependent auxotrophs and characterization of deficient *arg* genes in *L. plantarum*. Appl. Environ. Microbiol. **69:**2674–2683.
8. **Ebbole, D. J., and H. Zalkin.** 1989. *Bacillus subtilis pur* operon expression and regulation. J. Bacteriol. **171:**2136–2141.
9. **Elagöz, A., A. Abdi, J. C. Hubert, and B. Kammerer.** 1996. Structure and organisation of the pyrimidine biosynthesis pathway genes in *Lactobacillus plantarum*: a PCR strategy for sequencing without cloning. Gene **182:**37–43.
10. **Ghim, S. Y., C. C. Kim, E. R. Bonner, J. N. D'Elia, G. K. Grabner, and R. L. Switzer.** 1999. The *Enterococcus faecalis pyr* operon is regulated by autogenous transcriptional attenuation at a single site in the 5′ leader. J. Bacteriol. **181:**1324–1329.
11. **Ghim, S. Y., and J. Neuhard.** 1994. The pyrimidine biosynthesis operon of the thermophile *Bacillus caldolyticus* includes genes for uracil phosphoribosyltransferase and uracil permease. J. Bacteriol. **176:**3698–3707.
12. **Hammer-Jespersen, K., and A. Munch-Petersen.** 1973. Mutants of *Escherichia coli* unable to metabolize cytidine: isolation and characterization. Mol. Gen. Genet. **126:**177–186.
13. **Hughes, L. E., D. A. Beck, and G. A. O'Donovan.** 2005. Pathways of pyrimidine salvage in *Streptomyces*. Curr. Microbiol. **50**:8–10.
14. **Kaczanowska, M., and M. Ryden-Aulin.** 2005. The YrdC protein—a putative ribosome maturation factor. Biochim. Biophys. Acta **1727:**87–96.
15. **Kilstrup, M., and J. Martinussen.** 1998. A transcriptional activator, homologous to the *Bacillus subtilis* PurR repressor, is required for expression of purine biosynthetic genes in *Lactococcus lactis*. J. Bacteriol. **180:**3907–3916.
16. **Martinussen, J., P. Glaser, P. S. Andersen, and H. H. Saxild.** 1995. Two genes encoding uracil phosphoribosyltransferase are present in *Bacillus subtilis*. J. Bacteriol. **177:**271–274.
17. **Martinussen, J., and K. Hammer.** 1994. Cloning and characterization of *upp*, a gene encoding uracil phosphoribosyltransferase from *Lactococcus lactis*. J. Bacteriol. **176:**6457–6463.
18. **Martinussen, J., J. Schallert, B. Andersen, and K. Hammer.** 2001. The pyrimidine operon *pyrRPB-carA* from *Lactococcus lactis*. J. Bacteriol. **183:**2785–2794.
19. **Matthews, R. G.** 1996. One-carbon metabolism, p. 600–611. *In* F. C. Neidhardt, R. Curtiss III, J. L. Ingraham, E. C. C. Lin, K. B. Low, B. Magasanik, W. S. Reznikoff, M. Riley, M. Schaechter, and H. E. Umbarger (ed.), *Escherichia coli* and *Salmonella*: cellular and molecular biology, 2nd ed. ASM Press, Washington, D.C.
20. **Morishita, T., and M. Yajima.** 1995. Incomplete operation of biosynthesis and bioenergetic functions of the citric acid cycle in multiple auxotrophic lactobacilli. Biosci. Biotechnol. Biochem. **59:**251–255.
21. **Na, J. G., I. Pinto, and M. Hampsey.** 1992. Isolation and characterization of SUA5, a novel gene required for normal growth in *Saccharomyces cerevisiae*. Genetics **131:**791–801.
22. **Neuhard, J.** 1983. Utilization of preformed pyrimidine bases and nucleosides, p. 95–148. *In* A. Munch-Petersen (ed.), Metabolism of nucleotides, nucleosides and nucleobases in microorganisms. Academic Press, London, United Kingdom.
23. **Neuhard, J., and R. A. Kelln.** 1996. Biosynthesis and conversion of pyrimidines, p. 580–599. *In* F. C. Neidhardt, R. Curtiss III, J. L. Ingraham, E. C. C. Lin, K. B. Low, B. Magasanik, W. S. Reznikoff, M. Riley, M. Schaechter, and H. E. Umbarger (ed.), *Escherichia coli* and *Salmonella*: cellular and molecular biology. American Society for Microbiology, Washington, D.C.
24. **Nicoloff, H., F. Arsène-Ploetze, C. Malandain, M. Kleerebezem, and F. Bringel.** 2004. Two arginine repressors regulate arginine biosynthesis in *Lactobacillus plantarum*. J. Bacteriol. **186:**6059–6069.
25. **Nicoloff, H., and F. Bringel.** 2003. IS*Lpl1* is a functional IS*30*-related insertion element in *Lactobacillus plantarum* that is also found in other lactic acid bacteria. Appl. Environ. Microbiol. **69:**5832–5840.
26. **Nicoloff, H., A. Elagöz, F. Arsène-Ploetze, B. Kammerer, J. Martinussen, and F. Bringel.** 2005. Repression of the *pyr* operon in *Lactobacillus plantarum* prevents its ability to grow at low carbon dioxide levels. J. Bacteriol. **187:**2093–2104.
27. **Nicoloff, H., J.-C. Hubert, and F. Bringel.** 2000. In *Lactobacillus plantarum*, carbamoyl phosphate is synthesized by two carbamoyl-phosphate synthetases (CPS): carbon dioxide differentiates the arginine-repressed from the pyrimidine-regulated CPS. J. Bacteriol. **182**:3416–3422.
28. **Saxild, H. H., K. Brunstedt, K. I. Nielsen, H. Jarmer, and P. Nygaard.** 2001. Definition of the *Bacillus subtilis* PurR operator using genetic and bioinformatic tools and expansion of the PurR regulon with *glyA*, *guaC*, *pbuG*, *xpt-pbuX*, *yqhZ-folD*, and *pbuO*. J. Bacteriol. **183:**6175–6183.
29. **Schumacher, M. A., D. Carter, D. M. Scott, D. S. Roos, B. Ullman, and R. G. Brennan.** 1998. Crystal structures of *Toxoplasma gondii* uracil phosphoribosyltransferase reveal the atomic basis of pyrimidine discrimination and prodrug binding. EMBO J. **17:**3219–3232.
30. **Teplova, M., V. Tereshko, R. Sanishvili, A. Joachimiak, T. Bushueva, W. F. Anderson, and M. Egli.** 2000. The structure of the *yrdC* gene product from *Escherichia coli* reveals a new fold and suggests a role in RNA binding. Protein Sci. **9:**2557–2566.
31. **Tomchick, D. R., R. J. Turner, R. L. Switzer, and J. L. Smith.** 1998. Adaptation of an enzyme to regulatory function: structure of *Bacillus subtilis* PyrR, a *pyr* RNA-binding attenuation protein and uracil phosphoribosyltransferase. Structure **6:**337–350.
32. **Turner, R. J., Y. Lu, and R. L. Switzer.** 1994. Regulation of the *Bacillus subtilis* pyrimidine biosynthetic (*pyr*) gene cluster by an autogenous transcriptional attenuation mechanism. J. Bacteriol. **176:**3708–3722.